GEOPHYSICAL RESEARCH LETTERS, VOL. 27, NO. 15, PAGES 2301-2304, AUGUST 1, 2000

Did stress triggering cause the large off-fault aftershocks of the 25 March 1998 M_W=8.1 Antarctic plate earthquake?

Shinji Toda

Earthquake Research Institute, University of Tokyo, Japan

Ross S. Stein

U.S. Geological Survey, Menlo Park, California

Abstract. The 1998 Antarctic plate earthquake produced clusters of aftershocks ($M_W \leq 6.4$) up to 80 km from the fault rupture and up to 100 km beyond the end of the rupture. Because the mainshock occurred far from the nearest plate boundary and the nearest recorded earthquake, it is unusually isolated from the stress perturbations caused by other earthquakes, making it a good candidate for stress transfer analysis despite the absence of near-field observations. We tested whether the off-fault aftershocks lie in regions brought closer to Coulomb failure by the main rupture. We evaluated four published source models for the main rupture. In fourteen tests using different aftershocks sets and allowing the rupture sources to be shifted within their uncertainties, 6 were significant at $\geq$ 99% confidence, 3 at > 95% confidence, and 5 were not significant (< 95% level). For the 9 successful tests, the stress at the site of the aftershocks was typically increased by 1-2 bars (0.1-0.2 MPa). Thus the Antarctic plate event, together with the 1992 M_W=7.3 Landers and its M_W=6.5 Big Bear aftershock 40 km from the main fault, supply evidence that small stress changes might indeed trigger large earthquakes far from the main fault rupture.

Introduction

The 25 March 1998 M_W=8.1 Antarctic plate earthquake is one of the largest oceanic strike-slip events ever recorded. In addition to its spectacular size, the earthquake has two unique characteristics that motivate our study. The first is that the mainshock occurred about 250 km from the nearest plate boundary (Fig. 1), and 100 km from the nearest Figure 1 earthquake (a M_W=5.6 event in 1981) recorded by the Harvard CMT and ISC catalogs since their inception in 1976 and 1966, respectively. The presumed left-lateral fault is also at a high angle to the left-lateral transform boundary (Fig. 1), suggesting that the stress driving the Antarctic plate fault is not a product of plate boundary motion. For these reasons, the site of the 1998 shock is likely to be unusually isolated from the stress transfer from large nearby earthquakes or plate edges.

The other remarkable attribute of the Antarctic plate event is that its aftershocks are distributed over an extent of 350 km, with the largest M_W=6.4 event striking 100 km from of the mainshock and 80 km south of the inferred fault rupture (Fig. 1). Such large distant aftershocks or coupled mainshocks are not unknown. The 1812 $M_W \sim 7.5$ Wrightwood, California, earthquake on the San Andreas fault was followed 13 days later by the $M_W \sim 7.1$ Santa Barbara shock 200 km away; *Deng and Sykes* [1996] argued that the second shock was brought closer to Coulomb failure by the first. Most recently, the 1992 M_W=7.3 Landers earthquake was followed 3.5 hrs later by the M_W=6.5 Big Bear shock 40 km away. *King et al.* [1994] argued that the Big Bear shock was promoted by the 2-bar stress change associated with the Landers rupture. In many respects, the Antarctic plate event appears to be a larger version of the Landers-Big Bear sequence.

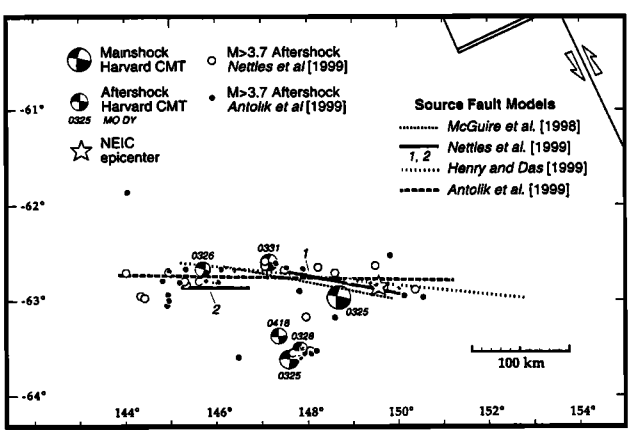

Figure 1. Map of the 1998 Antarctic plate mainshock and largest relocated aftershocks ($m_b \geq 3.7$). The rift-transform boundary of the Antarctic and Australian plates is visible in the northeast corner of the map. The rupture planes for the five tested models, in the positions given by their authors, are depicted by the bold lines.

Paper number 1999GL011129.
0094-8276/00/1999GL011129$05.00

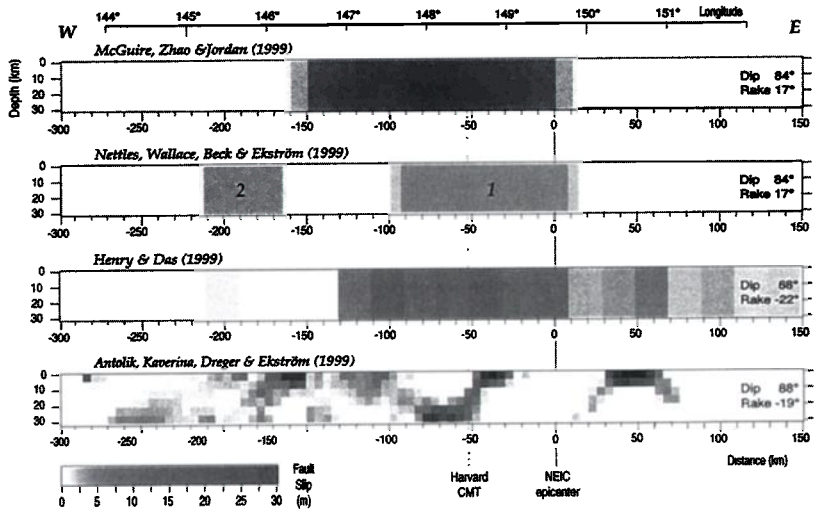

Figure 2. Slip functions for the rupture planes shown in Fig. 1, with the dip and rake indicated for each model. The width for all but the *Antolik et al.* model is set to 30 km.

The absence of near-field observations of the Antarctic plate earthquake adds uncertainty to any conclusions one can draw about the stress transfer. Teleseismic waveform modeling yields source parameters, slip functions, and aftershock locations. However, the fault width is unconstrained, and there are 15-25 km uncertainties in the location of the fault rupture with respect to the NEIC epicenter or CMT centroid, and 5 km uncertainties in the location of the aftershocks with respect to the mainshock [*Nettles et al.*, 1999; *Antolik et al.*, 1998]. The nominal uncertainty of the NEIC epicenter listed in the PDE phase data catalog is 8 km at 90% confidence, but this is likely an underestimate [*M. Nettles, written comm.*]; here we will use 15 km.

Methods and Assumptions

We calculate the static Coulomb failure stress change, which is expressed as $\Delta\sigma_f = \Delta\tau - \mu\Delta\sigma$, where $\Delta\tau$ is the shear stress change resolved on a given failure plane (reckoned positive in the direction of fault slip), $\Delta\sigma$ is the normal stress change (positive in compression) and μ is the coefficient of friction. Positive values of the Coulomb stress change are interpreted to promote failure, negative values to inhibit failure. We compute stress changes in an elastic halfspace [*Okada*, 1992] with a shear modulus of $3.2 \times 10^{10}\mathrm{Nm}^{-2}$ and a Poissons ratio of 0.25. See *King et al.* [1994], *Harris et al.* [1995], and *Harris* [1998] for discussion of the method.

For the Antarctic plate earthquake, we consider source models of *McGuire et al.* [1998], *Nettles et al.* [1999], *Henry and Das* [in prep.], and *Antolik et al.* [1999]. The faults are shown in Fig. 1, and slip functions in Fig. 2. Figure 2 All but *McGuire et al.* [1998] constrained their source to pass through the NEIC epicenter, and all show a concentration of slip near the CMT centroid (Fig. 2). *Nettles et al.* [1999] found two main subevents separated by 125 km, the first subevent having twice the moment of the second, so we also consider the possibility that the second subevent was triggered 60 sec later by static stress transfer from the first.

While the rupture length is determined in each source model by waveform inversion, the fault width (its down-

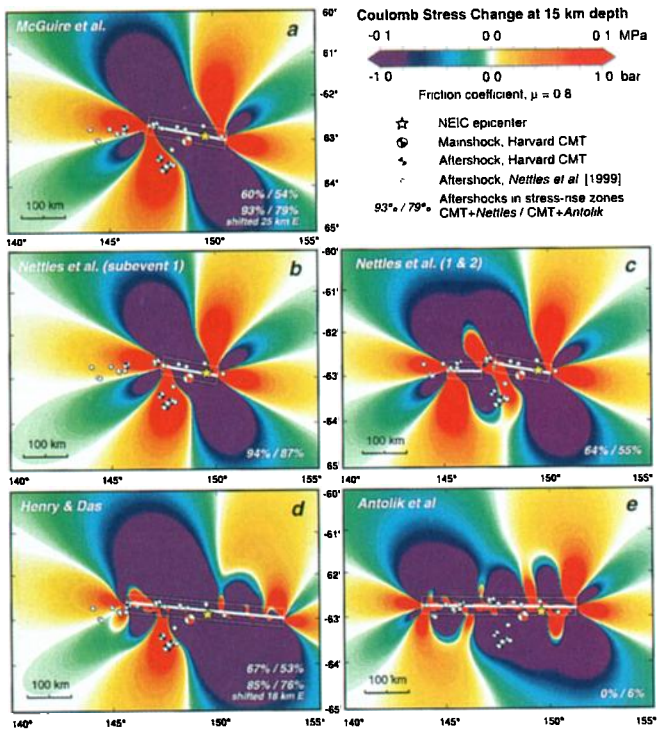

Figure 3. Calculated static stress change for the five source models. The percentage of CMT and either *Nettles et al.* or *Antolik et al.* relocated aftershocks falling in regions of Coulomb stress increase is also shown. Only aftershocks more than 20 km from the model fault plane (outside of the white box) are counted; thus the total number of shocks differs for each model. The *McGuire et al* and *Henry and Das* models are shown shifted east by the amounts indicated.

dip dimension) is poorly constrained. The width is important for our study because the fault length-to-width ratio controls the intensity of the lobes of stress increase off the slipped fault. A long rupture relative to its width, such as the Great 1906 San Francisco earthquake, drops the stress off the fault, whereas a short fault produces intense off-fault lobes in which failure is promoted [*King et al.*, 1994]. Here we set the fault width of all but the variable-depth *Antolik et al.* [1999] model to 30 km for the following reasons. The oceanic crust is 35-55 my old at the site of the Antarctic plate earthquake [*Müller et al.*, 1997]. Such an age yields a 27-38 km depth of the $700 - 800°$ isotherm [*Parsons and Sclater*, 1977], which *Wiens and Stein* [1983, 1984] found corresponds to the thickness of the seismogenic lithosphere. In addition, if the fault width were less than 15-20 km, the slip would be unrealistically high. *Wells and Coppersmith* [1994], for example, report 11 m as the peak observed slip in M_W=8 continental strike-slip events, whereas a width of 15 km would yield a mean slip of 25 m for the Antarctic event. We calculate the stress changes at a depth of 15 km, half the fault width, although our sensitivity tests indicate that the stress patterns are largely unchanged at depths of 5-25 km.

To assess the spatial association between aftershocks and the calculated static stress changes, we use the locations of the five largest aftershocks from the Harvard CMT catalog, as well as the locations of 17 $m_b \geq 3.7$ aftershocks from *Nettles et al.* [1999] using JHD relocations with residuals less than 3.5 sec; and 31 $m_b \geq 3.9$ events from *Antolik et al.* [1999] using a 3D earth model. We resolve the Coulomb stress changes on vertical, left-lateral faults striking 275°, the average strike of the left-lateral nodal plane of the mainshock and the five largest aftershocks (Fig. 1). We consider only aftershocks more than 20 km from the source, because at lesser distances, the stress change depends on the distribution of slip at scale of $\sim$ 10 km, which is unknown.

Results

Calculated Coulomb stress changes are sensitive to the assumed friction coefficient. Friction controls the distribution of the Coulomb stress change off the fault. As μ increases, the off-fault lobes grow in size and shift toward the dilatant quadrants, where faults are unclamped. We set $\mu = 0.8$ because a high value of friction fits the aftershocks distribution best. Friction of 0.8 is consistent with laboratory experiments for dry rock samples [*Byerlee et al.*, 1996]. In a stress-transfer study, *Parsons et al.* [1999] found that $\mu \geq 0.8$ for faults that lacked significant cumulative slip, which is likely true for the Antarctic plate fault. In the presence of high fluid pressures or extensive fault gouge, however, μ could be as low as 0.0-0.2, in which case the southern aftershocks could not be explained as a consequence of static stress transfer.

Simple models of the Antarctic plate earthquake are consistent with the off-fault shocks being brought closer to failure. *McGuire et al.* [1998] inverted for the first and second central moments of the moment-rate distribution in space and time, constrained by the Harvard CMT solution. We explored a range of locations for the source fault consistent with the 25 km uncertainty relative to the CMT centroid given by *McGuire et al.* When the fault is shifted 25 km to the east, 93% of the Nettles et al. aftershocks and 79% of the *Antolik et al.* aftershocks located $\geq$ 20 km from the rupture lie in regions brought closer to failure (Fig. 3a). Some 87-94% of the aftershocks Figure 3 lie in regions brought closer to failure by the first subevent of *Nettles et al.*[1999] (Fig. 3b). In addition, the rupture surface of the second subevent in *Nettles et al.* is brought 0.5-2.0 bars (0.05-0.20 MPa) closer to failure by rupture of the first subevent (for this calculation, we resolved the stress changes on the 270° strike of the second subevent).

More detailed slip functions yield more diverse results, in which two models fit the aftershock distribution well, and one does not. When we consider both subevents of *Nettles et al.* [1999], 55-64% of the aftershocks lie in regions where stress is calculated to have increased (Fig. 3c). The 360-km-long variable slip model of *Henry and Das* [1999] produces the broadest stress shadow, although it displays western and southern off-fault zones similar to that of *McGuire et al.* [1998]. Some 53-67% of aftershocks lie in regions brought closer to failure; if the *Henry and Das* source is shifted 18 km to the east, within the 25-km location uncertainty, 76-85% of the aftershocks lie in regions brought closer to failure (Fig. 3d). Because of its more heterogeneous slip distribution (Fig. 2), the *Antolik et al.* [1999] model produces numerous off-fault lobes (Fig. 3e). In this model, faulting extends through the western aftershock cluster, and the southern cluster lies in the stress shadow. Thus, none of the off-fault aftershocks lie in regions brought closer to failure, regardless of the nodal plane used to resolve the stress changes.

Discussion and Conclusions

For all but the *Antolik et al.* model, 60-94% of the off-fault aftershocks lie in regions calculated to have been brought closer to failure by the main rupture. This percentage rises to 85-93% when two models are shifted 18-25 km eastward. Such latitude in the position of the fault rupture with respect to the aftershocks is within the relative location error of the source models (Fig. 1). The aftershock-stress association is, however, predicated on the assignment of a 30-km fault width, the assumption of a high coefficient of friction, and the assumption that the off-fault shocks slip on the E-W nodal plane, which we can not independently verify.

We therefore evaluated the significance of the aftershock-stress correlations with the equal-tails test of the null hypothesis that the association is random.

Here we explicitly take into account the degrees of freedom inherent in our modeling, which includes setting the friction coefficient, the fault width, the aftershock nodal plane, and for some correlations, shifting the location of the source. These tests were conducted with both the *Nettles et al* and the *Antolik et al* aftershock sets. There are fourteen tests on four source models. In six cases the correlations are significant at the ≥99% confidence level; these include the *McGuire et al.* model when shifted 25 km east (Fig. 3a); the *Nettles et al.* two-subevent model when shifted 18 km west; and the *Henry and Das* model when shifted 18 km east (Fig. 3d). The ≥99% confidence level for these source models are obtained when using either the *Nettles et al.* or *Antolik et al.* aftershocks. Three aftershock-stress change correlations are significant at the >95% level [*McGuire et al.*, unshifted; both subevents of *Nettles et al.*, unshifted (Fig. 3c); *Henry and Das*, unshifted], and five are not significant (<95%). Thus, most but not all of the tested Antarctic plate source models are consistent with off-fault and fault-end shocks being triggered by stress increases of more than 1-2-bars (0.l-0.2 MPa).

In contrast to the off-fault shocks, aftershocks along the source faults, or within 20 km of the model faults, are generally inconsistent with the areas of calculated Coulomb stress increase. This may be because the detailed pattern of slip–and thus the stress changes close to the faultis poorly resolved Another feature common to all the models is that there are few aftershocks in the northern off–fault lobe or the eastern fault-end lobe (Fig. 3). We speculate that the secular stresses buildup at the transform plate boundary (Fig. 1) may inhibit failure to the northeast of the Antarctic plate shock.

In summary, the extraordinary distribution of aftershocks of the Antarctic plate event may be a product of static stress transfer. This possibility is tempered by the need to make several assumptions that cannot be fully verified. The Antarctic plate and Landers-Big Bear sequences together suggest that the seismic hazard posed by large aftershocks off the main fault can be assessed by stress-transfer calculations. In both the California and Antarctic events, aftershocks struck in regions brought 1-2 bars (0.1-0.2 MPa) closer to failure, and the time lags between mainshock and the largest aftershocks are short, 9.0 and 3.5 hours, respectively. The implications of such large and distant aftershocks for San Andreas ruptures are provocative: A great earthquake on the southern San Andreas fault might, for example, trigger a large aftershock on the urban Newport-Inglewood fault, potentially causing more damage than the mainshock.

Acknowledgments. We thank Meredith Nettles for encouraging us to undertake this study; M. Antolik, S. Das, G. Ekström, C. Henry, J. McGuire, and M. Nettles, for generously allowing us to use their unpublished preliminary source models; and J. McGuire, R. Harris and T. Parsons for thoughtful and incisive reviews of the manuscript. We are grateful to *Pacific Gas & Electric Co.* for funding this research.

References

Antolik M., A. Kaverina, D. Dreger, and G. Ekström, Finite fault rupture models of the 25 March, 1998 (Mw=8.2) Balleny Sea earthquake (abstract), *Eos Trans. AGU, 79*(45), Fall Meet. Suppl., F662, 1998.

Byerlee, J.D., Friction of rocks, *Pure Applied Geophys., 116,* 615-626, 1978.

Deng J., and L. R. Sykes, Triggering of 1812 Santa Barbara earthquake by a great San Andreas shock: Implications for future seismic hazards in southern California, *Geophys. Res. Lett., 23,* 115-1158, 1996.

Harris, R. A., Introduction to special section: Stress triggers, shadows, and implications for seismic hazard, *J. Geophys. Res., 103,* 24,347-24,358, 1998.

Harris, R. A., R. W. Simpson, and P. A. Reasenberg, Influence of static stress changes on earthquake locations in southern California, *Nature, 375,* 221-224, 1995.

Henry C., and S. Das, Rupture history of the 25th March, 1998, Balleny Islands earthquake (abstract), *Eos Trans. AGU, 79*(45), Fall Meet. Suppl., F662, 1998.

King G. C. P., R. S. Stein, and J. Lin, Static stress changes and the triggering of earthquakes, *Bull. Seismol. Soc. Am., 84,* 935-953, 1994.

McGuire, J. J., L. Zhao, and T. H. Jordan, GSDF inversion for higher moments of the stress glut rate tensor (abstract), *Eos Trans. AGU, 79* (45), Fall Meet. Suppl., F658, 1998.

Müller, R. D.. W. R. Roest, J.-Y. Royer, L. M. Gagagan, and J. G. Sclater, Digital isochrons of the worlds ocean floor, *J. Geophys. Res., 102,* 3211-3214, 1997.

Nettles M., T. C. Wallace, and S. Beck, The March 25, 1998 Antarctic plate earthquake, *Geophys. Res. Lett., 26,* 2097-2100, 1999.

Okada, Y., Internal deformation due to shear and tensile faults in a half space, *Bull. Seismol. Soc. Am., 82,*1018-1040, 1992.

Parsons, B., and J. G. Sclater, An analysis of the variation of ocean floor bathymetry and heat flow with age, *J. Geophys. Res., 82,* 803-827, 1977.

Parsons, T., R. S. Stein, R. W. Simpson, and P. A. Reasenberg, Stress sensitivity of fault seismicity: A comparison between limited-offset oblique and major strike-slip faults, *J. Geophys. Res., 104,* 20183-20202, 1999.

Stein R. S., G. C. P. King, and J. Lin, Stress triggering of the 1994 M=6.7 Northridge, California, earthquake by its predecessors, *Science, 265,* 1432-1435, 1994.

Wells, D. L., and K. J. Coppersmith, New empirical relationships among magnitude, rupture length, rupture width, rupture area, and surface displacement, *Bull. Seismol. Soc. Am., 84,* 974-1002, 1994.

Wiens, D. A., and S. Stein, Age dependence of oceanic intraplate seismicity and implications for lithospheric evolution, *J. Geophys. Res., 88,* 6455-6468, 1983

Wiens, D. A., and S. Stein, Intraplate seismicity and stresses in young oceanic lithosphere, *J. Geophys. Res., 89,* 11442-11464, 1984.

S. Toda, Earthquake Research Institute, University of Tokyo, Yayoi 1-1-1, Bunkyo-ku, Tokyo 113-0032, Japan. (e-mail: toda@eri.u-tokyo.ac.jp)

R. S. Stein, U.S. Geological Survey, 345 Middlefield Road, MS 977, Menlo Park, CA 94025. (e-mail: rstein@usgs.gov)

(Received October 20, 1999; revised January 28, 2000; accepted February 10, 2000.)